Thermodynamics of Polymer Melts Swollen with Supercritical Gases

Ashok Garg, Esin Gulari,* and Charles W. Manke

Department of Chemical Engineering and Materials Science and Institute for Manufacturing Research, Wayne State University, Detroit, Michigan 48202

Received October 12, 1993; Revised Manuscript Received May 31, 1994®

ABSTRACT: We report gas solubilities in molten polymers for two systems: the solubility of carbon dioxide in poly(dimethylsiloxane) and the solubility of 1,1-difluoroethane in polystyrene are measured in the range of temperatures and pressures where the gas is supercritical. The solubility data are correlated by two lattice-theory-based equations of state, namely, the Sanchez–Lacombe and Panayiotou–Vera equations of state, which employ a single adjustable binary interaction parameter. Both equations of state provide satisfactory descriptions of the solubility data when the binary interaction parameter is allowed to depend on temperature. The utility of the mixture equations of state is illustrated by predictions of swollen volume, isothermal compressibility, and thermal expansion coefficient for the mixtures over the range of data.

Introduction

The knowledge of gas solubility and the effects of dissolved gases on the physical properties of a polymer melt, such as swollen volume, isothermal compressibility, and thermal expansion coefficient, are important in various polymer processing operations. Volatile components are present in many polymer applications, and they are of central importance to operations such as foam processing. Dense gases or supercritical fluids also have a great potential as a unique class of solvents or processing aids for molten polymers that can act to reduce melt viscosity.

Dissolved gases can reduce the viscosity of molten polymers significantly through two mechanisms. The first mechanism is the dilution of chain entanglements within the melt when a solvent is added. The second mechanism involves generating additional free volume which increases chain mobility; this mechanism depends directly on the mixture density. In the case of dissolved gases, both mechanisms contribute, and the second mechanism can greatly enhance the viscosity reduction, as shown by Gerhardt et al.[1] A key to the basic understanding of this useful viscosity reduction is accurate estimation of the composition and density of the gas–polymer mixtures over a wide range of temperatures and pressures, including both subcritical and supercritical regions of gas PVT behavior.

For a given gas–polymer system, appreciable levels of gas solubility are achieved when the polymer is molten, above its glass transition temperature T_g, and when the gas is dense or supercritical. Solubility and thermodynamic data for dense and supercritical gases in molten polymers are scarce, as documented by several review papers.[2,3] However, studies of diffusivities and solubilities of gases across solid polymer films have been reported[4–6] at pressures near or slightly above ambient pressures. In as much as the polymers are in their glassy or crystalline state and the gases are not dense, these data cannot be readily extrapolated to higher pressures and temperatures. Several investigations of the solubilities of polymers in supercritical fluids have also been reported,[7–9] but in these cases the emphasis is on controlling fractionation and selectivity in the separation of polydisperse polymers into narrow molecular weight fractions. Data from these studies pertain to relatively dilute solutions of low molecular weight polymers dissolved in supercritical fluids. Therefore, a gap exists in available data for dense gas solubilities in high molecular weight polymer melts, and the results presented here attempt to bridge this gap.

We present solubility data for two systems: carbon dioxide in poly(dimethylsiloxane) (PDMS) (MW = 308 000) and 1,1-difluoroethane (R152a) in polystyrene (MW = 165 000). For the first system, solubility data have been obtained at 50, 80, and 100 °C over a pressure range of 0–26 MPa. The T_g of PDMS is −127 °C, and T_c and P_c of carbon dioxide are 31.3 °C and 7.2 MPa, respectively. Thus PDMS is approximately 200 °C above its T_g, and CO_2 is supercritical over a range of our experimental conditions. PDMS is a viscous liquid at ambient temperatures with rheological behavior similar to that of many other high molecular weight molten polymers at their processing temperatures; therefore, it is a convenient ambient temperature analog to thermoplastic melts.

For the polystyrene–1,1-difluoroethane system, solubility data have been obtained at 135 and 160 °C over a pressure range of 0–17 MPa. The T_g of polystyrene is 106 °C, and T_c and P_c of 1,1-difluoroethane are 113.4 °C and 4.5 MPa, respectively. Thus, polystyrene is about 20–50 °C above its T_g, and 1,1-difluoroethane is supercritical over a range of the experimental conditions. Unlike PDMS, which is far above its T_g in the first set of measurements, polystyrene is only slightly above its T_g in the second set.

Prior Solubility Measurements. Silicone polymers have many applications ranging from coatings to implants to hydraulic fluids, and several studies of the solubilities of gases in silicone polymers are available. The solubilities of volatile solvents in PDMS have been measured by a gas–liquid chromatographic technique[10–13] in which the specific retention volume of the volatile solvent is determined using a chromatographic column packed with a polymer-coated support. This method yields values of Henry's law constant, the solubility parameter, and other thermodynamic properties accurately, but the data are limited to near-ambient pressures. The solubility of carbon dioxide in a specially formulated silicone oil [(trifluoropropyl)methylsiloxane] at elevated pressures was reported by Wedlake and Robinson.[14] They observed surprisingly high CO_2 solubility (up to 47% by weight) at 6 MPa and 22 °C. Fleming and Koros[15] studied the dilation of cross-linked silicone rubbers by sorption of carbon dioxide at 35 °C and at pressures up to 6 MPa using mass sorption/desorption measurements. Shah et al.[16,17] com-

® Abstract published in *Advance ACS Abstracts*, August 15, 1994.

0024-9297/94/2227-5643$04.50/0

pared the solubility of several gases (carbon dioxide, methane, and propane) in several silicone polymers and studied the effects of polymer chain structure. They concluded that the substitution of methyl chains by bulkier groups decreases the solubility of the gases in PDMS. Their results are restricted to 10–55 °C and 0–3 MPa.

Data are also available for the solubility of gases in polystyrene. The high-pressure data include that of Newitt and Weale[18] for hydrogen, nitrogen, ethylene, and carbon dioxide at 191 °C and 0–30 MPa; Lundberg et al.[19–21] for methane at 100–188 °C and 30 MPa and nitrogen at 125–226 °C and 70 MPa; Durill and Griskey[22,23] for nitrogen, helium, carbon dioxide, and argon at 188 °C and 2 MPa; Stiel and Harnish[24] for several hydrocarbons and freons at 135–230 °C and 0.4 MPa; and Wissinger and Paulaitis[25,26] for carbon dioxide at 33–65 °C and pressures up to 10 MPa. The gases employed in these studies have critical temperatures significantly lower than the glass transition temperature of polystyrene, leading to relatively low solubility. For example, many of the data for polystyrene have been obtained using carbon dioxide, but since the T_c of CO_2 (31.3 °C) is much lower than T_g (106 °C) of polystyrene, only limited solubilities are observed when the polymer is molten.[18,22,23]

Thermodynamic Modeling. The choice of an appropriate thermodynamic model to adequately describe systems containing a polymer melt with dissolved gas or a supercritical fluid is complicated because the two components are quite dissimilar. Since the polymer is the major component in a swollen melt, a viable strategy is to choose a lattice model that describes the pure polymer melt satisfactorily. Such models, though not ideally suited for gases, can also yield adequate descriptions of the upper phase (essentially pure gas), thereby enabling use of the same equation of state for both phases. Thus, a consistent method for predicting the properties of the lower phase mixture can be developed. Kiszka et al.[27] have used the Sanchez–Lacombe (S–L) equation of state (EOS) to fit the solubility data of several binary systems (carbon dioxide–PMMA, ethane–LDPE, methane–polystyrene), whereas Wissinger and Paulaitis[25,26] used the Panayiotou–Vera (P–V) equation of state (for carbon dioxide in PMMA and polystyrene). Both models employ a single adjustable parameter for binary interactions, and both models have achieved reasonable success in the studies cited. The success of these two lattice models provides a motivation for us to employ the S–L and the P–V EOS's to correlate our high-pressure solubility data. We also present the model predictions for temperature, pressure, and composition dependences of various thermodynamic properties derivable from the EOS, such as swollen volume, isothermal compressibility, and thermal expansion coefficient of the polymer–gas mixture.

Experimental Procedure

Solubility measurements were performed by charging polymer and gas to a temperature-controlled pressure vessel and allowing the mixture to equilibrate under continuous stirring. All experiments were performed under conditions that produced a polymer-rich lower phase in equilibrium with an upper phase consisting essentially of pure gas. These phases were allowed to separate under gravity, and a small sample of the lower phase was withdrawn for compositional analysis. A sketch of the apparatus used for solubility measurements is shown in Figure 1.

A typical experiment is initiated by charging the pressure vessel, a Parr Instruments reactor Model 4572, with about 1 L of polymer and loading the gas, by means of a high-pressure generator, to the desired pressure (prior to pressurization, the air space is purged with gas at low pressure). During the

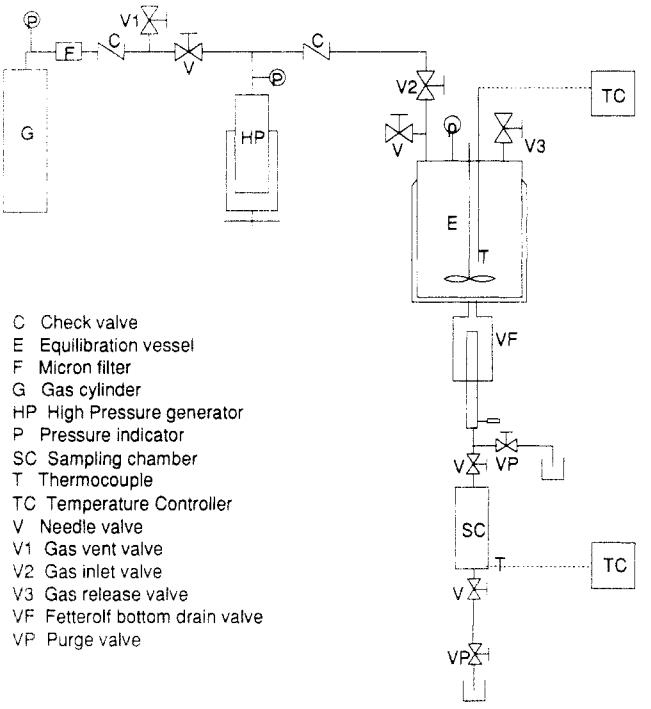

Figure 1. Experimental apparatus for solubility measurements.

experiment, the vessel pressure is measured by a pressure transducer with ±0.007 MPa resolution and a temperature controller maintains the system to within ±0.5 °C of the set point. The vessel contents are stirred continuously during equilibration, and the pressure decreases as gas dissolves into the polymer. Attainment of equilibrium, which occurs after several hours of stirring, is indicated by the pressure leveling to a constant value. A detachable sampling chamber with a capacity of 2.97 mL, connected to the outlet of the sampling valve, is used to collect a representative sample of the lower phase at the system temperature and pressure. The sampling chamber is then detached, and its contents are analyzed.

The amount of gas present in the sample is determined by depressurizing the sample and collecting the evolved gas in a cylinder of gas-saturated water at ambient conditions. The gas content is then determined by measuring the displaced volume. The PDMS content is evaluated by dissolving the degassed polymer in a known volume of toluene and measuring the PDMS concentration of this solution by FTIR spectrocopy. The PDMS signature peak at 1261.5 cm^{-1} due to a $Si-CH_3$ stretch is used for FTIR analysis. The calibration curves are established by comparing the PDMS signature peak to three characteristic toluene peaks at 895.52, 1179.1, and 1210.4 cm^{-1} for known standard solutions. The calibration curves are linear and have similar slopes over the entire concentration range of the measurements (see ref 28 for further details).

In the polystyrene–1,1-difluoroethane experiments, the gas content is determined by volumetric displacement, as described above, and the polystyrene content is determined gravimetrically.

Materials. The PDMS (MW = 308 000 and viscosity 10^6 cSt) was obtained from Petrarch Systems, Inc. Samples of polystyrene of molecular weight 165 000 have been supplied by Dow Chemicals. Carbon dioxide (99% bone dry) from Scott Specialty Gases and 1,1-difluoroethane (CH_3CHF_2, Freon R152a) from Du Pont Chemicals are used without further purification.

EOS Models

Our group[28,29] and other groups[25–27] have successfully used the lattice theory equations of state to correlate thermodynamic properties and phase behavior of polymer/SCG systems. In this study, we correlate solubility of carbon dioxide in PDMS and 1,1-difluoroethane in polystyrene by employing two lattice-theory-based equations of state: the Sanchez–Lacombe (S–L) equation of state,[30–32] which is derived from Flory–Huggins theory,

and a modified version suggested by Panayiotou and Vera (P–V)[33,34] that incorporates concepts developed by Guggenheim.

Sanchez–Lacombe (S–L) Equation of State.[30–32] The S–L equation of state is given by:

$$\frac{\tilde{P}}{\tilde{T}} = -\ln(1-\tilde{\rho}) - \left(1-\frac{1}{r}\right)\tilde{\rho} - \frac{\tilde{\rho}^2}{\tilde{T}} \tag{1}$$

where $\tilde{\rho}$, $\tilde{P}$, and $\tilde{T}$ are reduced density, pressure, and temperature, respectively. The reduced variables are defined in terms of characteristic parameters:

$$\tilde{T} = T/T^* \qquad T^* = \epsilon^*/R$$

$$\tilde{P} = P/P^* \qquad P^* = \epsilon^*/v^* \tag{2}$$

$$\tilde{\rho} = \rho/\rho^* \qquad \rho^* = M/(rv^*)$$

where T^*, P^*, and ρ^* are characteristic temperature, pressure, and density, respectively. The parameter ϵ^* is the interaction energy, v^* is the characteristic volume of a lattice site, and r is the number of lattice sites occupied by a molecule of molecular weight M. In the Sanchez–Lacombe theory, T^*, P^*, and ρ^* are derived from ϵ^*, v^*, and r, as shown in eq 2. In application of the S–L EOS, however, T^*, P^*, and ρ^* are often determined directly as the pure component parameters by an optimization procedure.

The EOS for the mixture is formally identical to that of a pure component. However, mixing rules are employed for calculating the characteristic parameters and r of the mixture. In formulating the mixing rules, two material balance equations for the close-packed mixture are introduced. The first balance represents the conservation of the close-packed molecular volume of each component and can be expressed as $r_i v^* = r_i^\circ v_i^*$. This relationship guarantees that an i molecule occupying r_i° sites of volume v_i^* in its pure state will occupy the same volume, r_i sites of volume v^* in the mixture. The second rule keeps the total number of pair interactions in the close-packed mixture the same as the sum of the pair interactions of the components in their pure close-packed states, i.e., $\sum_i r_i^\circ N_i = rN$ where N_i is the number of i molecules and N is the total number of molecules in the lattice.

The combined result of these material balances is to introduce a surface area effect so that a component in a binary mixture with a larger mer volume can have more interactions in the mixture than in its pure state. The average close-packed mer volume in the mixture is defined by:

$$v^* = \sum_i \phi_i^\circ v_i^* \tag{3}$$

where $\phi_i^\circ = r_i^\circ N_i/\sum_i(r_i^\circ N_i)$ is the close-packed volume fraction of component i in the mixture. The average number of lattice sites occupied by the mixture, r, is weighted by mole fractions:

$$r = \sum_i x_i r_i \tag{4}$$

The characteristic pressure P^* of the mixture is taken as pairwise additive:

$$P^* = \sum_i \sum_j \phi_i \phi_j P_{ij}^*; \quad P_{ij}^* = (P_i^* P_j^*)^{1/2}(1-\delta_{ij}) \tag{5}$$

where ϕ_i is the volume fraction of component i in the mixture, given by $\phi_i = r_i N_i/\sum_i(r_i N_i)$. The binary interaction parameter δ_{ij}, the only mixture parameter, corrects the deviation of the mixture's P_{ij}^* from the geometric mean of components' characteristic pressures, P_i^* and P_j^*. In the application of the EOS to a binary or pseudobinary mixture, v^*, r, and P^* for the mixture are calculated from eqs 3–5 and then the other three parameters ϵ^*, T^*, and ρ^* are determined from the relationships given in eq 2.

The phase equilibrium is defined by equating the chemical potentials of gas in the two phases: $\mu_1^G(T,P) = \mu_1^P(T,P,\phi_i)$ where the superscripts G and P represent the gas and polymer phases, respectively; the subscript 1 represents the lighter component (gas). The upper phase is assumed to be pure. The difference of the chemical potentials of component 1 in the two phases, which must vanish at equilibrium, is given by:

$$\frac{\Delta\mu_1}{RT} = 0 = \ln\phi_1 + \left(1-\frac{r_1}{r_2}\right)\phi_2 + r_1^\circ \tilde{\rho} X_1 \phi_2^2 + \tilde{v}\tilde{\rho}\ln\tilde{\rho} - \tilde{v}_1\tilde{\rho}_1\ln\tilde{\rho}_1 + r_1^\circ\left[-\frac{\tilde{\rho}-\tilde{\rho}_1}{\tilde{T}_1} + \frac{\tilde{P}_1(\tilde{v}-\tilde{v}_1)}{\tilde{T}_1} + \tilde{v}(1-\tilde{\rho})\ln(1-\tilde{\rho}) - \tilde{v}_1(1-\tilde{\rho}_1)\ln(1-\tilde{\rho}_1)\right] \tag{6}$$

where $X_1 = (P_1^* + P_2^* + 2P_{12}^*)v_1^*/RT$ is the only parameter containing δ_{ij}.

Panayiotou–Vera Equation of State.[34] Panayiotou and Vera obtain their equation of state from the partition function for a distribution of molecules and holes on a quasilattice with constant lattice site volume v_H and a finite coordination number Z. For pure components, a random distribution of molecules and holes is assumed and the equation of state is given by:

$$\frac{\tilde{P}}{\tilde{T}} = \ln\left(\frac{\tilde{v}}{\tilde{v}-1}\right) + \frac{Z}{2}\ln\left(\frac{\tilde{v}+q/r-1}{\tilde{v}}\right) - \frac{\theta^2}{\tilde{T}} \tag{7}$$

where $\tilde{P}$, $\tilde{T}$, and $\tilde{v}$ are reduced pressure, temperature, and volume, respectively. The reduced variables are related to each other in terms of characteristic parameters

$$\frac{Z}{2}\epsilon = P^* v_H = RT^*$$

$$\tilde{v} = \frac{V}{V^*} = \frac{v_{sp}}{v_{sp}^*}; \quad \tilde{T} = \frac{T}{T^*}; \quad \tilde{P} = \frac{P}{P^*} \tag{8}$$

The effective chain length q and the number of lattice sites r occupied by a molecule are related by:

$$qZ = (Z-2)r + 2 \tag{9}$$

where r is determined from the definition of hard-core volume ($V^* = Nrv_H$).

The parameter θ is the fraction of the total external contacts in the system that are mer–mer contacts in a random array of molecules and holes. It is explicitly defined in terms of effective chain length and the number of lattice sites occupied by a given component as $\theta_i = Zq_iN_i/ZN_q$ where N_q is the total number of external contacts present in the system. If N_0 denotes the number of holes, then $N_q = N_0 + \sum_i q_i N_i$. This formal and explicit introduction of θ_i makes P–V different from the S–L equation, where the surface contactness is implied by the mixing rules.

In the P–V EOS, the characteristic energy of a component is considered to be temperature dependent because it represents an average value over all possible configurations of the system. The total energy of a molecule is then given by the sum of enthalpic and entropic contributions ($\epsilon = \epsilon_h + T\epsilon_s$).

Three parameters are required for complete characterization of a pure fluid. The parameters ϵ_s (entropic contribution to interaction energy), ϵ_h (enthalpic contribution to interaction energy), and v_{sp}^* (characteristic hard-core volume) are determined from pure component data. The other parameters q, r, T^*, and P^* are calculated from eqs 8 and 9.

The mixture equation of state is formally identical to that for a pure component, except that nonrandom distributions of molecules are considered, which leads to modification of some of the parameters. The mixing rules for the P–V equation evaluate q and r as linear averages weighted by mole fractions, whereas the mixture energy reflects the effects of nonrandom distributions:

$$q = \sum_i x_i q_i$$

$$r = \sum_i x_i r_i \tag{10}$$

$$\epsilon^* = \bar{\theta}_1\epsilon_{11} + \bar{\theta}_2\epsilon_{22} - \bar{\theta}_1\bar{\theta}_2\Gamma_{12}\Delta\epsilon$$

The molecular surface fraction $\bar{\theta}_i$ accounts for the nonrandom distribution of holes and molecules on the lattice and is given by $\bar{\theta}_i = Zq_iN_i/ZqN = \theta_i/\theta$, where the total number of external contacts is simply the sum of the contacts for individual mers ($\theta = \sum_i\theta_i$, $\theta_0 = 1 - \theta$).

For a binary system, Γ_{11}, Γ_{22}, and Γ_{12} are nonrandom factors and are related by a simple material balance equation

$$\bar{\theta}_1\Gamma_{11} + \bar{\theta}_2\Gamma_{12} = \bar{\theta}_2\Gamma_{22} + \bar{\theta}_1\Gamma_{12} = 1 \tag{11}$$

$$\Gamma_{12} = \frac{2}{1 + [1 - 4\bar{\theta}_1\bar{\theta}_2(1 - G)]^{1/2}} \tag{12}$$

$$G = \exp\left(\theta\frac{\Delta\epsilon}{RT}\right), \quad \Delta\epsilon = \epsilon_{11} + \epsilon_{22} + 2\epsilon_{12} \tag{13}$$

where the term ϵ_{12} incorporates δ_{ij}, the adjustable binary interaction parameter used to account for deviation of the characteristic energy of the mixture from the geometric mean of individual components' characteristic energies. In P–V, δ_{ij} is introduced as a correction for the binary interaction energy ($\epsilon_{12} = (\epsilon_{11}\epsilon_{22})^{1/2}(1 - \delta_{ij})$), while the binary interaction term δ_{ij} in S–L modifies the additivity of characteristic pressures and thus has a different physical meaning.

At equilibrium, the chemical potentials of the gas in the two phases are equal: $\mu_1^G(T,P) = \mu_1^P(T,P,x_i)$. The difference of the chemical potential of component 1 in the mixture (polymer phase) and the chemical potential of pure gas at the same temperature and pressure is given by:

$$\frac{\Delta\mu_1}{RT} = 0 = \ln\phi_1 + \ln\frac{\tilde{v}_1}{\tilde{v}} + q_1\ln\left(\frac{\tilde{v}}{\tilde{v}-1}\frac{\tilde{v}_1 - 1}{\tilde{v}_1}\right) + q_1\left(\frac{2\theta_{1,p} - \theta}{\tilde{T}_1} - \frac{\theta}{\tilde{T}}\right) + \frac{Zq_1}{2}\ln\Gamma_{11} \tag{14}$$

where Γ_{11} is related to the material balance of nonrandom factors (eq 11). $\theta_{1,p}$ refers to the surface fraction of pure component 1 at the same conditions, and ϕ_1 is the volume fraction of component 1:

$$\phi_1 = \theta_1\frac{\tilde{v} + q/r - 1}{q_1/r_1} \tag{15}$$

Comparison of EOS Models. Both Sanchez–Lacombe and Panayiotou–Vera equations of state are based on modeling the fluid as essentially a solidlike structure. However, there are several basic differences between the two models: the S–L model is similar to the original Flory–Huggins theory, employing an infinite coordination number approximation in the mathematical development, but the lattice contains occupied and unoccupied sites, with site volumes that are component dependent. In the development of the P–V EOS, a finite coordination number and a constant site volume are used, and the treatment of nonrandom distribution of occupied sites is introduced through Guggenheim's quasichemical approximation. Consequently, the concept of surface fractions appears explicitly in the P–V EOS, while it emerges implicitly from the mixing rules for the S–L EOS. The parametrization of the two EOS's in their application to pure component PVT data and the mixing rules used in calculating mixture properties are totally different, as described in the previous section. Thus, a rigorous comparison of the two models is difficult.

In correlating the gas solubility data, we use the EOS first to describe pure component PVT data, thereby establishing all pure component EOS parameters. Next, vapor–liquid equilibria are computed by matching the chemical potentials of the gas in the upper and lower phases. In this second step, the binary interaction parameter δ_{ij} is optimized to yield the best description of solubility data. Therefore, a reasonable scheme for comparing S–L and P–V EOS's is first to test how well the pure component PVT data are described by the EOS with the optimized pure component parameters. We then examine how both models describe solubility data for our two experimental systems. Finally, we examine the composition dependence of the S–L and P–V predictions for the chemical potential of the gas in the mixture and thereby identify any possible differences between the two models in describing the free energy of the lower phase mixtures.

Determination of Pure Component Parameters. In general, polymers are relatively incompressible, and compressibility data are limited to a relatively narrow range of densities. The pure component parameters recommended by Sanchez and Lacombe[32] and Panayiotou and Vera,[34] listed in Table 1, are used in our calculations. As shown in Figure 2, both the S–L and P–V models describe PVT data of pure PDMS very satisfactorily.

In contrast, the gas is highly compressible and exists over a wide range of densities. The pure component parameters depend on the particular range of gas PVT data selected for parameter optimization. A logical approach is to include PVT data over the widest ranges of temperature, pressure, and specific volume that are available in the literature. The pure component parameters optimized for such data are suitable for a wide range of temperature and pressure conditions. This strategy differs from that of other research groups, who determine optimum pure component parameters to match PVT data within a relatively narrow range of pressure–temperature conditions selected to correspond specifically to their experiments. While narrow-range parametrization may

Table 1. Pure Component Parameters Used for Thermodynamic Calculations

Sanchez–Lacombe EOS

component	T^* (K)	P^* (MPa)	ρ^* (g/cm³)	T_c^{EOS} (K)	P_c^{EOS} (MPa)
carbon dioxide (I)[a]	328.1	464.2	1.426	318.4	9.42
carbon dioxide (II)[b]	330.4	458.0	1.430	319.1	9.53
PDMS[32]	476.0	302.0	1.104		
1,1-difluoroethane[a]	402.7	366.4	1.206	405.8	6.45
polystyrene[32]	735.0	357.0	1.105		

Panayiotou–Vera EOS

component	ϵ_h (cal/mol)	ϵ_s (cal/(mol K))	v_{sp}^* (cm³/g)	T_c^{EOS} (K)	P_c^{EOS} (MPa)
carbon dioxide (I)[a]	189.817	−0.0934	0.7689	311.2	12.12
carbon dioxide (II)[b]	168.807	−0.0202	0.8950	325.6	11.32
PDMS[34]	133.130	0.1450	0.8911		
1,1-difluoroethane[a]	172.756	0.0187	0.8939	406.2	7.75
polystyrene[34]	167.540	0.2220	0.8801		

[a] Optimization based on pressure. [b] Optimization based on volume.

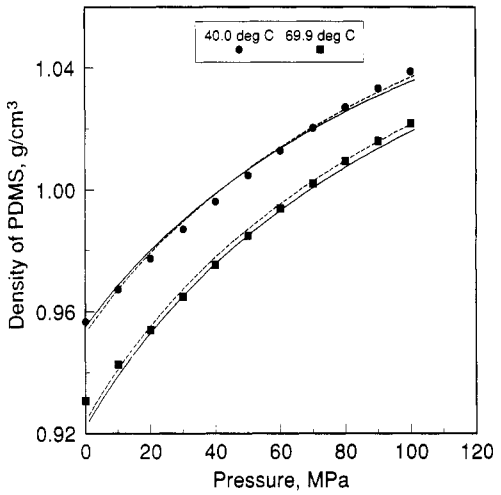

Figure 2. Comparison of experimental densities of PDMS[40] with the values predicted by Sanchez–Lacombe and Panayiotou–Vera equations of state at two temperatures. The solid lines represent S–L fits (T^* = 476.0 K, P^* = 302.0 MPa, and ρ^* = 1.104 g/cm³), and the dashed lines denote P–V fits (ϵ_h = 133.130 cal/mol, ϵ_s = 0.145 cal/(mol K), and v_{sp}^* = 0.8911 g/cm³).

provide a better local description of the pure component PVT data, locally optimized parameters may be quite unreliable in extrapolations to different temperature and pressure conditions.

For gases, the three pure component parameters required for the S–L EOS, ρ^*, T^*, and P^*, and the parameters for the P–V EOS, ϵ_h, ϵ_s, and v_{sp}^*, are obtained by fitting each EOS to the pure component PVT data. We have employed either pressure or the specific volume in forming an object function SSQ for minimization. Our optimization routine is based on minimizing

$$\mathrm{SSQ} = \sum_i [(\tilde{P}/\tilde{T})^{EOS} - (\tilde{P}/\tilde{T})^{exp}]^2 \quad \text{or} \quad \mathrm{SSQ} = \sum_i [(v^{exp} - v^{EOS})/v^{exp}]^2 \quad (16)$$

We use a modified Levenberg–Marquardt algorithm and a finite difference Jacobian for minimizing eq 16, thereby determining the pure component parameters. Carbon dioxide PVT data from Michels and co-workers[35–37] over a pressure range of 0–300 MPa and a temperature range of 0–150 °C are used to evaluate parameters for carbon dioxide. The data of Iso and Uematsu[38] for 1,1-difluoroethane over a pressure range of 0–10 MPa and a temperature range of 45–130 °C are used in the calculation of 1,1-difluoroethane parameters. These results are listed in Table 1.

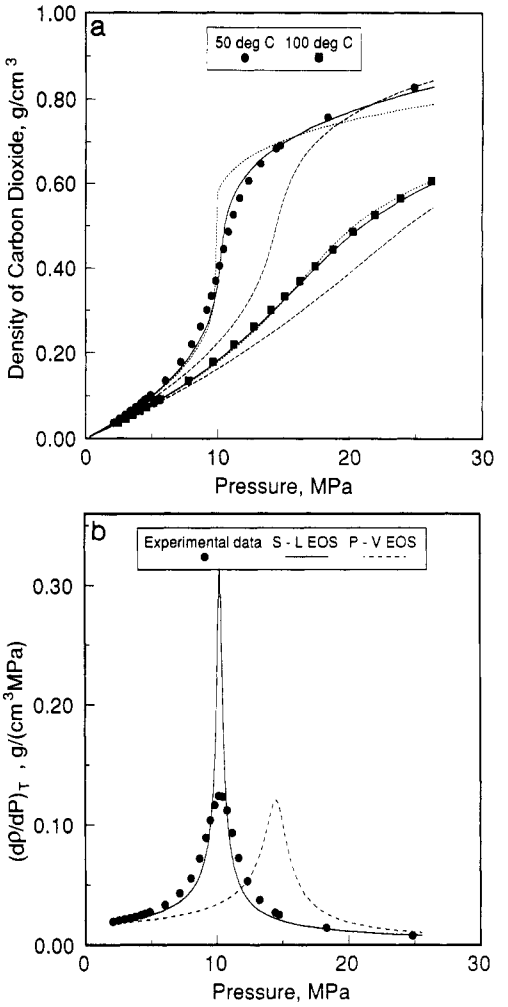

Figure 3. (a) Comparison of measured densities of carbon dioxide[35,36] with the values predicted by Sanchez–Lacombe and Panayiotou–Vera equations of state. The solid lines represent S–L fits (T^* = 328.1 K, P^* = 464.2 MPa, and ρ^* = 1.426 g/cm³), the dashed lines denote P–V fits based on "pressure" optimization (ϵ_h = 189.817 cal/mol, ϵ_s = −0.0934 cal/(mol K), and v_{sp}^* = 0.7689 g/cm³), and the dotted lines denote P–V fits based on "volume" optimization (ϵ_h = 168.807 cal/mol, ϵ_s = −0.0202 cal/(mol K), and v_{sp}^* = 0.8950 g/cm³). (b) Comparison of $(\partial\rho/\partial P)_T$ of carbon dioxide calculated from measured densities[35,36] with the values predicted by Sanchez–lacombe and Panayiotou–Vera equations of state along the 50 °C isotherm of Figure 3a. The solid lines represent predictions of the S–L, and the dashed lines represent predictions of the P–V model. Pressure-optimized parameters, listed in Table 1, were used for both models.

In Figure 3a, carbon dioxide density data along two isotherms are compared with S–L and P–V EOS predictions that employ the pure component parameters listed in Table 1. We find that the optimum set of characteristic parameters for the S–L model, ρ^*, T^*, and P^*, correspond to a well-defined minimum in the ρ–T–P space; if the object function for the minimization procedure is changed from pressure to specific volume, ρ^*, T^*, and P^* values are affected very little. However, the characteristic parameters for the P–V EOS cannot be determined uniquely because the ϵ_h and ϵ_s values compensate each other, with the total interaction energy remaining constant for a range of ϵ_h and ϵ_s values. Depending on the object function for minimization, variations in v_{sp}^* values are also observed. Clearly, the S–L model predictions are in very good agreement with data along the two isotherms illustrated

in Figure 3a, while there is only fair agreement between the data and the P–V model predictions.

The markedly superior carbon dioxide density predictions of the S–L model along the 50 °C isotherm in Figure 3a would seem to suggest that the S–L EOS description of the gas phase is generally superior to the P–V description. However, an examination of two other important properties of the gas phase leads us to the opposite conclusion. First, we examine the critical properties of carbon dioxide as predicted by the S–L and P–V EOS's. Predicted critical properties for both pressure-optimized and volume-optimized parameters are listed in Table 1. The P–V volume-optimized parameters are rejected because they produce unrealistic two-phase behavior along the 50 °C isotherm; therefore, pressure-optimized parameters are used for all subsequent P–V model predictions. The true critical point of carbon dioxide is 304.2 K and 7.2 MPa, whereas the predicted critical values are 318.4 K and 9.4 MPa according to the S–L EOS and 311.2 K and 12.12 MPa according to P–V EOS. Both models deviate substantially from the true critical pressure of carbon dioxide, but the P–V prediction is much closer to the true critical temperature than S–L. We expect this difference to be important along the 50 °C isotherm, which is close to the critical temperature.

In Figure 3b, we examine a second property related to compressibility, namely, the partial derivative $(\partial\rho/\partial P)_T$ that measures the change in density with pressure. The S–L model follows the experimental data well except near 10 MPa, where a large overshoot occurs in the model predictions. Large $(\partial\rho/\partial P)_T$ values are characteristic of the critical region, where $(\partial\rho/\partial P)_T \rightarrow \infty$ at the critical point, and the presence of extremely high $(\partial\rho/\rho P)_T$ values in the S–L predictions at 50 °C is an artifact of the error in the predicted critical temperature. The P–V predictions reflect the magnitude and trend of the data well, although the predictions are shifted about 5 MPa higher in the pressure, which corresponds to the difference between the predicted P_c and the true P_c. The P–V curve does not exhibit the unrealistic overshoot seen in the S–L predictions. For these reasons, we conclude that the P–V model exhibits more realistic behavior for carbon dioxide than S–L, in spite of the excellent S–L density predictions at 50 °C.

Results and Discussion

Solubility Experiments. The measured solubility of carbon dioxide in PDMS of nominal molecular weight 308 000 at 50, 80, and 100 °C is plotted in Figures 4 and 5, and the solubility of 1,1-difluoroethane in polystyrene of molecular weight 165 000 at 135 and 160 °C is shown in Figures 6 and 7, along with equation of state descriptions of the data, which are discussed later. The solubility data represent the compositional analyses of lower phase samples collected after equilibrium has been established for several hours, as indicated by the cessation of the pressure fluctuations that accompany gas dissolution. As noted earlier, the upper phase is taken to be pure gas. This assumption is supported by GPC analysis of the polymer,[28] in which volatile, low molecular weight fractions are absent from the elution curves. The absence of polymer in the upper phase is further confirmed by the absence of any polymer deposits on the gas vent after decompression of the reactor contents.

The qualitative features of the solubility data are typical of solubility isotherms at conditions above the critical temperature of the gas. An "S"-shaped isotherm is observed with an inflection point in the vicinity of the

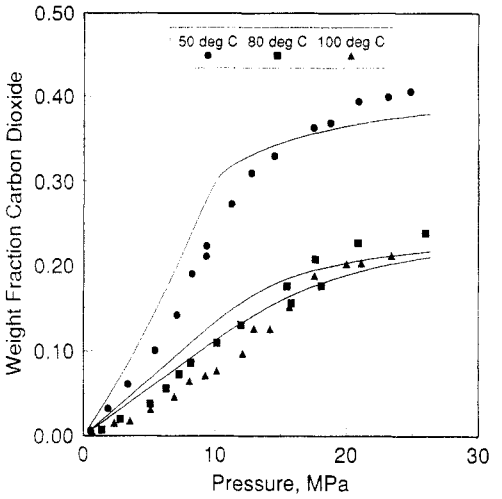

Figure 4. Solubility of carbon dioxide in PDMS. The solid curves represent predictions of the Sanchez–Lacombe equation of state with parameters listed in Tables 1 and 2.

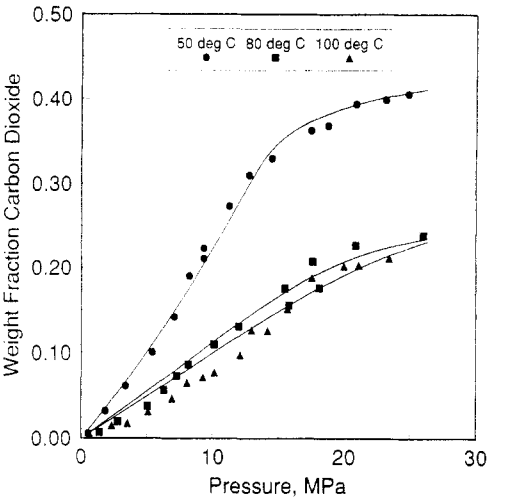

Figure 5. Solubility of carbon dioxide in PDMS. The solid curves represent predictions of the Panayiotou–Vera equation of state with parameters listed in Tables 1 and 2.

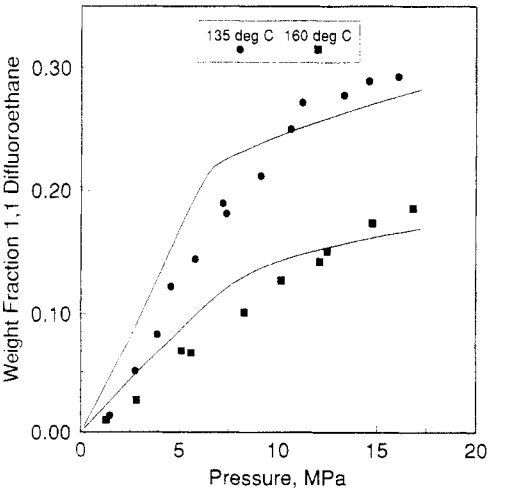

Figure 6. Solubility of 1,1-difluoroethane in polystyrene. The solid curves represent predictions of the Sanchez–Lacombe equation of state with parameters listed in Tables 1 and 2.

critical pressure. At 50 °C and at the highest experimentally available pressure (about 26 MPa), carbon dioxide solubility in PDMS is about 40% by weight. At higher temperatures, the solubility is reduced, but even the CO_2 solubility of 20% by weight attained at high

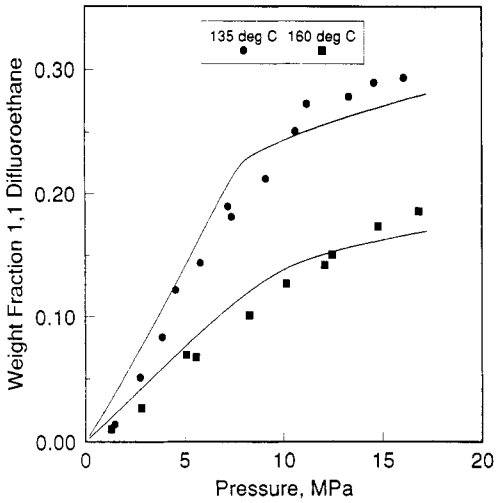

Figure 7. Solubility of 1,1-difluoroethane in polystyrene. The solid curves represent predictions of the Panayiotou–Vera equation of state with parameters listed in Tables 1 and 2.

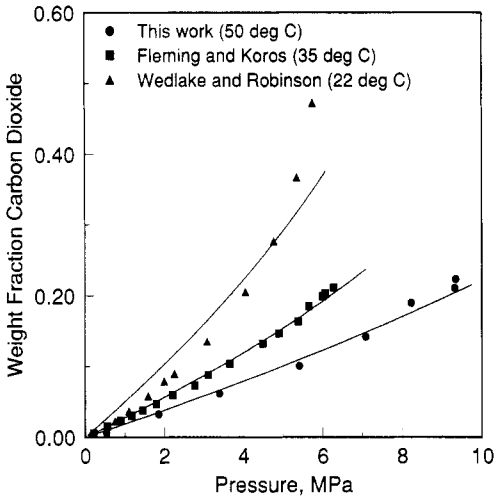

Figure 8. Comparison of the solubility of carbon dioxide in different grades of silicone polymers. The solid curves represent predictions of the Panayiotou–Vera equation of state. The value of δ_{ij} is 0.130 for this work (50 °C), 0.097 for Fleming and Koros[15] (35 °C), and 0.036 for Wedlake and Robinson[14] (22 °C).

pressures along the 100 °C isotherm would be sufficient to induce significant changes in the flow properties of the molten polymer. Similarly, solubilities of 15–30% by weight, depending upon temperature and pressure, for 1,1-difluoroethane in polystyrene would produce significant and useful viscosity reduction in polymer processing applications.

Our solubility measurements for the PDMS–CO_2 system complement solubility data for carbon dioxide in other silicone polymers obtained previously by other groups. Wedlake and Robinson[14] measured the solubility of carbon dioxide in (trifluoropropyl)methylsiloxane (Dow Corning silicone oil FS-1265), and Fleming and Koros[15] measured the solubility of CO_2 in cross-linked silicone rubber at 35 °C. In Figure 8, the solubility data from refs 14 and 15 are compared to our data, along with isotherms predicted by the P–V EOS. All three data sets are similar, and it is interesting to note that the solubility isotherms exhibit a strikingly consistent pattern of dependence on temperature and pressure, in spite of differences in the polymer molecular weights and the presence of cross-linking, or different end groups, on the polymer chains. The isotherms predicted by the P–V EOS fit the data well, with the largest deviations appearing at 22 °C, where more complicated phase behavior may occur because the temperature is below T_c of CO_2.

Table 2. Binary Interaction Parameters for Experimental Systems

polymer	gas	temp (°C)	binary interaction parameter, δ_{ij} S–L EOS	P–V EOS
PDMS	carbon dioxide	50	0.075	0.130
		80	0.122	0.180
		100	0.128	0.182
polystyrene	1,1-difluoroethane	135	0.034	0.039
		160	0.064	0.064

EOS Solubility Predictions. We use Sanchez–Lacombe and Panayiotou–Vera equations of state to model our gas–polymer solubility data, subject to the following assumptions: (1) The measured solubilities of gas in the polymer represent equilibrium conditions, (2) above the glass transition temperature, the polymer melt can be treated as a liquid (the CO_2–PDMS data are taken about 180–230 °C above T_g of PDMS and the 1,1-difluoroethane–polystyrene data are taken about 30–55 °C above T_g of polystyrene), and (3) the solubility of the polymer in the upper phase is negligible.

The Sanchez–Lacombe and Panayiotou–Vera equations of state are fitted to the solubility data using identical methodologies. The pure component characteristic parameters (ρ^*, P^*, and T^* for S–L and ϵ_h, ϵ_s, and v_{sp}^* for P–V EOS) listed in Table 1 are used for all calculations. In addition to these pure component parameters, the EOS binary interaction parameters δ_{ij} must be evaluated for each isotherm to fully specify the mixture EOS. An iterative procedure was adopted to determine optimum δ_{ij} values at each experimental temperature. First, a trial value of δ_{ij} is adopted and the mixture EOS is solved for the predicted equilibrium lower phase composition at pressures corresponding to the measured points along the isotherm. This procedure involves simultaneous solution of eqs 1 and 6 for S–L, or eqs 7 and 14 for P–V, along with the evaluation of characteristic mixture parameters using eqs 3–5 or 10. The quality of the fit is assessed by calculating the sum of the squares of error, SSE, corresponding to the squared differences between the predicted compositions and the measured compositions along the isotherm. The value of δ_{ij} for the isotherm is continuously varied until the cumulative error is minimized, and the δ_{ij} value corresponding to the minimum in SSE is chosen as the optimum value for that particular isotherm. The optimized binary interaction parameters are given in Table 2. For both S–L and P–V, the relatively small values for δ_{ij}, particularly for polystyrene–1,1-difluoroethane, indicate that binary interactions follow the parameter mixing rules without strong departures due to specific interactions. Apart from this similarity, the δ_{ij}'s for the two models cannot be compared because they have completely different physical meanings.

The solubility isotherms corresponding to the δ_{ij} values in Table 2 are displayed in Figures 4 and 5 for PDMS–carbon dioxide and in Figures 6 and 7 for polystyrene–1,1-difluoroethane. The quality of the solubility isotherm fits is satisfactory and similar for both S–L and P–V EOS's at temperatures far away from the critical temperature of the gas, namely, the 80 and 100 °C isotherms shown in Figures 4 and 5 and the 160 °C isotherm shown in Figures 6 and 7. At temperatures close to the T_c of the gas, the 50 °C isotherm in Figures 4 and 5 and the 135 °C isotherm in Figures 6 and 7, a kink, or sharp change in slope, of the predicted solubility isotherm is frequently observed. These kinks may result from the large gas compressibilities

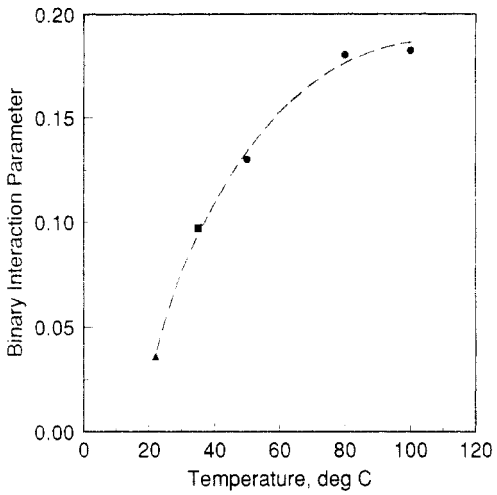

Figure 9. Effect of temperature on the P–V interaction parameter δ_{ij} for the CO_2–PDMS mixtures shown in Figure 8. Circles represent our data, the square represents the data of Fleming and Koros, and the triangle represents the data of Wedlake and Robinson.

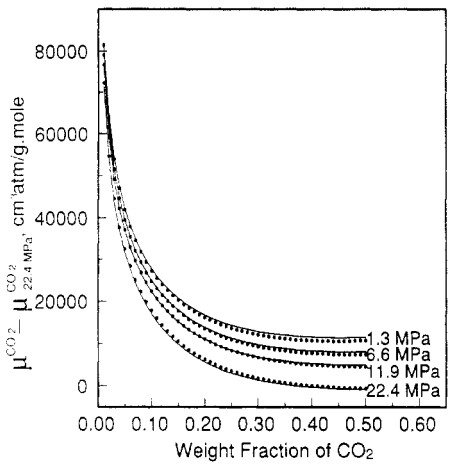

Figure 10. Chemical potential of carbon dioxide in lower phase PDMS–CO_2 mixtures displayed as a function of the lower phase composition at 50 °C. The solid lines represent the predictions of the S–L model, while the circles correspond to the P–V model. The chemical potential of pure CO_2 at 50 °C and 22.4 MPa is used as a reference state for both models.

near the critical point, which can produce abrupt changes in density over small pressure increments. Note that the 50 °C isotherm for PDMS–CO_2 shown in Figure 4 for the S–L model is kinked, whereas the comparable P–V isotherm shown in Figure 5, is not kinked. The corresponding carbon dioxide T_c for the S–L model, 45 °C, is very close to 50 °C, while the T_c predicted by P–V, 38 °C, is farther away. This issue is further discussed in the next section, where the differences between the S–L and P–V models in predicting the chemical potentials of the coexisting phases are compared.

The binary interaction parameters for both S–L and P–V models appear to be temperature dependent. For the P–V model, this dependence is shown in Figure 9, which is compiled from our data and data from the literature.[14,15] Although the measured solubilities can be satisfactorily described by a strictly empirical dependence of δ_{ij} on temperature, the strong dependence of δ_{ij} on the temperature indicates the need for developing a theoretical framework that incorporates this temperature dependence as a fundamental model feature.

Compositional Dependence of CO_2 Chemical Potential. Because the S–L and P–V models employ different parametrization and different mixing rules for calculating mixture properties, there does not seem to be any truly rigorous way of establishing equivalent parameter sets for comparison of these models. Here we have adopted the pure component parameters and optimized δ_{ij} values developed in the previous section as a practical basis for model comparisons. Under these conditions, the P–V model gives a markedly better description of the measured solubility isotherm at 50 °C for the PDMS–CO_2 system than the S–L EOS. Significant differences in the PVT behavior of pure CO_2 predicted by S–L and P–V are also seen at 50 °C, suggesting that the differences in the predicted solubility isotherms may be at least partly due to the EOS descriptions of the upper phase. To further investigate the reasons for these differences, we now examine the compositional dependence of CO_2 chemical potential in the mixed lower phase, as predicted by the two models. In Figure 10, the excess CO_2 chemical potentials predicted by the S–L and P–V models, referenced to the predicted values of chemical potential at 22.4 MPa (an arbitrarily selected high pressure where CO_2 exists as a dense gas), are plotted as a function of composition for four isobars in the pressure range of our solubility measurements at 50 °C. We obtain a very close correspondence between the two models, which indicates that both S–L and P–V models provide essentially identical descriptions of the lower phase. Therefore, the differences in the predicted solubility isotherms at 50 °C, shown in Figures 4 and 5, must be ascribed to differences in the predicted chemical potentials of the pure gas in the upper phase.

In describing the pure gas PVT data, both models predict values of T_c and P_c that are higher than the actual values, as indicated in Table 1. The apparent closeness to the critical point results in artificially high values of the predicted compressibilities along the 50 °C isotherm for CO_2 and the 135 °C isotherm for 1,1-difluoroethane. For example, at 50 °C for CO_2, the apparent $T - T_c$ is 5 °C for the S–L model and 12 °C for the P–V model, while the actual $T - T_c$, 19 °C, is much larger. Similarly, at 135 °C for 1,1-difluoroethane, the apparent $T - T_c$ is 2 °C for both models, while the true $T - T_c$ is 22 °C. The artifically high compressibility values, illustrated by the S–L curve in Figure 3b, enter into the phase equilibrium calculations through the evaluation and matching of the gas chemical potentials in the coexisting phases. Under these conditions, systematic deviations between the measured solubilities and model fits to the solubility isotherms are observed, as shown in Figure 4 along the 50 °C isotherm and in Figures 6 and 7 along the 135 °C isotherms. Since lattice theories such as S–L and P–V are intended as physical models for condensed polymeric systems rather than gases, the apparent advantage of P–V here, in describing critical properties of a pure gas upper phase (CO_2 at 50 °C), should be regarded as a purely empirical outcome. However, these comparisons do illustrate the importance of describing the upper phase accurately and the associated problems encountered in the critical region for any EOS.

Swollen Volume. When a polymer–gas mixture is modeled by an EOS with a specific binary interation parameter, other thermodynamic properties of the mixture can be calculated. We have used the P–V EOS, which describes the solubility data quite well for both of our experimental systems, to calculate various thermodynamic properties such as swollen volume, isothermal compressibility, and thermal expansion coefficient of polymer–gas mixtures. Parameters for these calculations are listed in Tables 1 and 2.

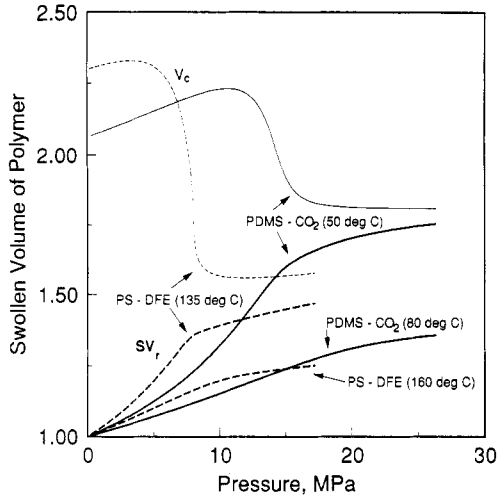

Figure 11. Swollen volumes for PDMS–CO_2 and PS–DFE systems. The heavier lines represent the real swollen volumes and lighter lines are the component volumes.

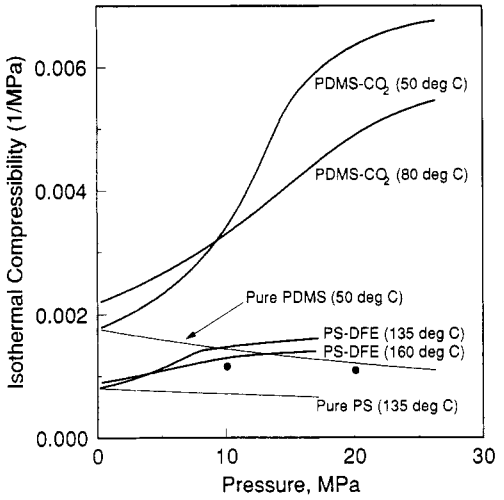

Figure 12. Isothermal compressibility β for PDMS–CO_2 and PS–DFE systems predicted by the Panayiotou–Vera equation of state. The heavier lines represent the mixture values, and the lighter lines represent pure polymers. The circles represent the isothermal compressibility of pure PDMS at 49.1 °C calculated from the data of Beret and Prausnitz.[40]

In molding or foaming of mixtures containing a polymer with dissolved gas under pressure, the swollen volume, i.e., the increased volume of the mixture in comparison to that of pure polymer, is an important property. Here swollen volume is represented by the specific volume of the mixture (obtained from the EOS) normalized by the fractional volume of polymer in the mixture; we call this ratio the "real" swollen volume ($SV_r = v/w_2v_2$). In Figure 11, SV_r is displayed as a function of pressure for the PDMS–CO_2 system at 50 and 80 °C and for the PS–DFE system at 135 and 160 °C. The sum of the pure component volumes, which are normalized in the same manner as SV_r, is called the component volume ($V_c = [w_1v_1 + w_2v_2]/w_2v_2$), which is also shown in Figure 11. The component volume V_c represents ideal volumetric mixing, and the difference between V_c and SV_r is due to the volume change upon mixing as gas is dissolved into the lower phase. Clearly, the changes in the mixture's swollen volume depend upon the amount of gas dissolved in the polymer. When the gas is subcritical, the swollen volume increases sharply with pressure as gas solubility increases. As pressure increases to supercritical values, the mixture becomes less compressible. In this regime, the real swollen volume approaches the sum of the volumes of the individual components. This observation indicates that, although the volume changes upon dissolution of gas into a polymer melt are highly nonideal at low pressures, the behavior tends toward ideal mixing at supercritical conditions.

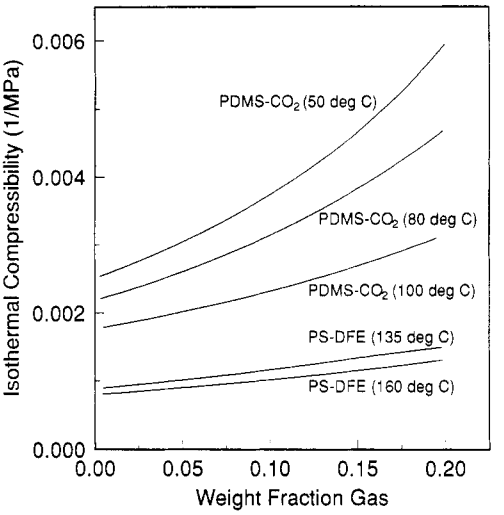

Figure 13. Concentration dependence of isothermal compressibility β for systems shown in Figure 13. The predictions are based on the Panayiotou–Vera equation of state.

Other Thermodynamic Properties. The isothermal compressibility, β, and the thermal expansion coefficient, α, are important properties in the processing of polymers. For pure polymer, closed-form expressions for β and α have been derived for both the S–L EOS[30] and P–V EOS.[34] Analogous closed-formed expressions are not available for mixtures; however, β and α can be calculated easily by numerical differentiation. The mixture's isothermal compressibility and thermal expansion coefficient were obtained here by employing a five-point numerical differentiation technique to calculate β and α from the following definitions:

$$\beta = -\frac{1}{V}\left[\frac{\partial V}{\partial P}\right]_{T,w_1} \tag{17}$$

$$\alpha = \frac{1}{V}\left[\frac{\partial V}{\partial T}\right]_{P,w_1} \tag{18}$$

Values for β calculated for pure polymer and for polymer–gas mixtures by the P–V EOS are plotted in Figure 12. For pure polymers, the predicted temperature and pressure dependences of isothermal compressibilities are as expected: the polymer becomes slightly less compressible as pressure is increased and it becomes slightly more compressible as temperature is increased, reflecting the changes in free volume with temperature and pressure.[39] The effect of dissolved gas on the compressibility of the mixture is significant. The β of the mixture increases with pressure because the amount of dissolved gas increases with pressure, but the pressure dependence of β along an isotherm is strongly influenced by both the amount and the compressibility of the gaseous component. When β is plotted as a function of equilibrium compositions rather than pressure, the isotherms do not exhibit the crossovers observed in Figure 12. In Figure 13, the dependence of the mixture's β on the gas content in the mixture is shown for both systems. PDMS–CO_2 mixtures exhibit appreciably higher compressibilities than PS–DFE mixtures because PDMS is about 200 °C above its T_g while polystyrene is only about 30 °C above its T_g under the conditions of these calculations.

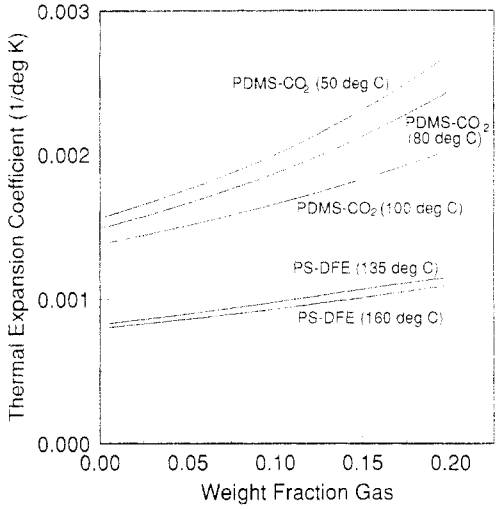

Figure 14. Concentration dependence of thermal expansion coefficients α for PDMS–CO_2 and PS-DFE predicted by the Panayiotou–Vera equation of state.

The coefficients of thermal expansion calculated for the mixture and the pure polymer show a similar behavior. For polymers swollen by gas, α increases significantly with pressure due to the increased gas solubility. The dependence of α on gas content behaves in a manner similar to that for β, yielding a simpler plot for w–α isotherms than the corresponding P–α isotherms. Figure 14 shows the coefficients of thermal expansion plotted as a function of composition of the equilibrated mixture. Once again, the PDMS–CO_2 mixtures exhibit much higher thermal expansion coefficients than PS–DFE because the isotherms are evaluated at temperatures much higher than the glass transition temperature of the polymer.

The values presented in Figures 11–14 are limiting values for gas-saturated mixtures; for operations at lower (undersaturated) gas concentrations, the values of swollen volumes, isothermal compressibility, and the coefficient of thermal expansion are correspondingly closer to the those of the pure polymer.

Conclusions

New data have been reported for gas solubility in two different molten polymer–gas systems at high temperatures and pressures. These measurements extend from near the Henry's law regime, where many previous experiments have been conducted, to the region of supercritical gas behavior, where data have been scarce. In both systems, PDMS–carbon dioxide and polystyrene–1,1-difluoroethane, S-shaped solubility isotherms are observed, showing significant enhancements in solubility as critical conditions are approached for the gas. Ultimately, very high solubilities (30–40% by weight) are attained at high pressures.

Solubility measurements for the PDMS–CO_2 system were quite similar to those reported previously for crosslinked silicone rubbers and functionally-substituted silicone polymers, except that the new measurements extend to substantially higher pressures. Remarkably, chemical differences and differences in molecular weight among these silicone polymers apparently have little effect on CO_2 solubility. All of the CO_2 solubility data for silicone liquids and silicone rubbers, including those taken in this study, are described adequately by the Panayiotou–Vera equation of state with a binary interaction parameter that is a smooth, monotonic function of temperature.

The extended temperature and pressure range of the current data provides an ideal opportunity for evaluating the ability of existing lattice theory equations of state, namely, the Sanchez–Lacombe EOS and the Panayiotou–Vera EOS, to model gas solubility in molten polymers. These theories are known to give excellent descriptions of the *PVT* behavior of pure molten polymers. They also provide at least an adequate description of the gas, thereby providing a single, consistent model for describing phase equilibrium for polymer–gas mixtures. With this approach, we obtain satisfactory comparisons of both the Sanchez–Lacombe EOS and the Panayiotou–Vera EOS to the solubility data for the PDMS–CO_2 and PS–DFE systems. At the same time, neither theory provides a perfect description, qualitatively or quantitatively, of gas solubility behavior over the entire range of pressure and temperature studied here.

While both the S–L and P–V theories are shown to be useful models for describing gas solubility in polymer melts at high pressures, the potential for improved thermodynamic modeling remains. The key to many of these improvements may be better modeling of the gas, rather than more sophisticated modeling of the polymer. Our comparison of the S–L and P–V models to the PDMS–CO_2 solubility data indicates that model predictions at high pressure are very sensitive to the model-predicted critical temperature of the gas. In the case of PDMS–CO_2, the P–V model appears to give better solubility predictions because the predicted critical temperature of CO_2 is closer to the actual T_c.

The utility of mixture equations of state, such as the S–L and the P–V models, for engineering purposes is illustrated by predictions of swollen volume, isothermal compressibility, and thermal expansion coefficients for the PDMS–CO_2 and the PS–DFE systems. These calculations realistically represent nonideal mixing effects that simpler models, or mixing rules, would fail to identify. Moreover, the difficulty of measuring these quantities experimentally over the wide ranges of conditions necessary for an empirical representation of thermodynamic properties would seem to cast the EOS approach used here as a very practical and attractive alternative.

Acknowledgment. The authors acknowledge the financial support of Michigan Materials Processing Institute and the NSF/State of Michigan/Industry–University–Cooperative Research Center of Michigan State University.

References and Notes

(1) Gerhardt, L.; Garg, A.; Bae, Y. C.; Manke, C. W.; Gulari, E. *Proceedings of the XIth International Congress on Rheology*; Moldenaers, P., Ed.; Elsevier: New York, 1992, p 348.
(2) Bonner, D. C. *Polym. Eng. Sci.* **1977**, *17*, 65.
(3) McHigh, M. A.; Krukonis, V. J. *Supercritical Fluid Extraction: Principles and Practice*; Butterworths: Boston, 1986.
(4) Pope, D. S.; Fleming, G. K.; Koros, W. J. *Macromolecules* **1990**, *23*, 2988.
(5) Vieth, W. R.; Laird, S. P. *J. Membr. Sci.* **1992**, *72*, 119.
(6) Vittoria, V.; Russo, F.; Ruvolo Filho, A. *J. Macromol. Sci., Phys.* **1993**, *B32*, 327.
(7) Saraf, V. P.; Kiran, E. *J. Supercrit. Fluids* **1988**, *1*, 37.
(8) Meilchen, M. A.; Hasch, B.; McHugh, M. A. *Macromolecules* **1991**, *24*, 4874.
(9) Kiran, E.; Zhuang, W.; Sen, Y. L. *J. Appl. Polym. Sci.* **1993**, *47*, 895.
(10) Flory, P. J.; Shih, H. *Macromolecules* **1972**, *5*, 761.
(11) Ashworth, A. J.; Price, G. J. *Macromolecules* **1986**, *19*, 358.
(12) Roth, M.; Novak, J. *Macromolecules* **1986**, *19*, 364.
(13) Price, G. J.; Guillet, J. E. *J. Solution Chem.* **1987**, *16*, 605.
(14) Wedlake, G. D.; Robinson, D. B. *J. Chem. Eng. Data* **1979**, *24*, 305.
(15) Fleming, G. K.; Koros, W. J. *Macromolecules* **1986**, *19*, 2285.
(16) Shah, V. M.; Hardy, B. J.; Stern, S. A. *J. Polym. Sci., Part B: Polym. Phys.* **1986**, *24*, 2033.

(17) Shah, V. M.; Hardy, B. J.; Stern, S. A. *J. Polym. Sci., Part B: Polym. Phys.* **1993**, *31*, 313.
(18) Newitt, D. M.; Weale, K. E. *J. Chem. Soc.* **1948**, 1541.
(19) Lundberg, J. L.; Wilk, M. B.; Huyett, M. J. *J. Appl. Phys.* **1960**, *31*, 1131.
(20) Lundberg, J. L.; Wilk, M. B.; Huyett, M. J. *J. Polym. Sci.* **1962**, *57*, 275.
(21) Lundberg, J. L.; Wilk, M. B.; Huyett, M. J. *Ind. Eng.* 4Chem. *Fundam.* **1963**, *2*, 37.
(22) Durill, P. L.; Griskey, R. G. *AIChE J.* **1966**, *12*, 1147.
(23) Durill, P. L.; Griskey, R. G. *AIChE J.* **1969**, *15*, 106.
(24) Stiel, L. I.; Harnish, D. F. *AIChE J.* **1976**, *22*, 117.
(25) Wissinger, R. G.; Paulaitis, M. E. *J. Polym. Sci., Part B: Polym. Phys.* **1987**, *25*, 2497.
(26) Wissinger, R. G.; Paulaitis, M. E. *Ind. Eng. Chem. Res.* **1991**, *30*, 842.
(27) Kiszka, M. B.; Meilchen, M. A.; McHugh, M. A. *J. Appl. Polym. Sci.* **1988**, *36*, 583.
(28) Garg, A. Ph.D. Dissertation, Wayne State University, Detroit, MI, 1993.
(29) Daneshvar, M.; Kim, S.; Gulari, E. *J. Phys. Chem.* **1990**, *94*, 2124.
(30) Sanchez, I. C.; Lacombe, R. H. *J. Phys. Chem.* **1976**, *80*, 2352.
(31) Lacombe, R. H.; Sanchez, I. C. *J. Phys. Chem.* **1976**, *80*, 2568.
(32) Sanchez, I. C.; Lacombe, R. H. *Macromolecules* **1978**, *11*, 1145.
(33) Panayiotou, C.; Vera, J. H. *Can. J. Chem. Eng.* **1981**, *59*, 501.
(34) Panayiotou, C.; Vera, J. H. *Polym. J.* **1982**, *14*, 681.
(35) Michels, A.; Michels, C. *Proc. R. Soc. London, Ser. A* **1936**, *153*, 201.
(36) Michels, A.; Michels, C.; Wouters, H. *Proc. R. Soc. London, Ser. A* **1936**, *153*, 215.
(37) Michels, A.; Blaisse, B.; Michels C. *Proc. R. Soc. London, Ser. A* **1937**, *160*, 358.
(38) Iso, A.; Uematsu, M. *Physica A* **1989**, *156*, 454.
(39) Ferry, J. D. *Viscoelastic Properties of Polymers*; Wiley: New York, 1980.
(40) Beret, S.; Prausnitz, J. M. *Macromolecules* **1975**, *8*, 536.